Selective Targeting of Antitumor Immune Responses with Engineered Live-Attenuated *Listeria monocytogenes*

Kiyoshi Yoshimura,[1,3] Ajay Jain,[1,2] Heather E. Allen,[4] Lindsay S. Laird,[1] Christina Y. Chia,[1] Sowmya Ravi,[1] Dirk G. Brockstedt,[4] Martin A. Giedlin,[4] Keith S. Bahjat,[4] Meredith L. Leong,[4] Jill E. Slansky,[5] David N. Cook,[4] Thomas W. Dubensky,[4] Drew M. Pardoll,[1] and Richard D. Schulick[1,2]

[1]Immunology and Hematopoiesis Division, Department of Medical Oncology, Sidney Kimmel Cancer Center; [2]Department of Surgery, Johns Hopkins Medical Institutions, Baltimore, Maryland; [3]Department of Surgery II, Yamaguchi University School of Medicine, Yamaguchi, Japan; [4]Cerus Corp., Concord, California; and [5]Department of Immunology, University of Colorado Health Sciences Center, Denver, Colorado

Abstract

Improved immunization and *ex vivo* T-cell culture strategies can generate larger numbers and more potent tumor-specific effector cells than previously possible. Nonetheless, the capacity of these cells to eliminate established tumors is limited by their ability to efficiently enter tumor-bearing organs and mediate their effector function. In the current study, we show that the administration of an engineered organ-homing microbe selectively targets tumor-specific immune responses to metastases within that organ. Specifically, an attenuated *Listeria monocytogenes* strain, which preferentially infects the liver following systemic administration, dramatically enhances the activity of a cancer vaccine against liver metastases but not metastases in the lung. This enhanced activity results from both local recruitment of innate immune effectors as well as concentration and increased activation of vaccine-induced antitumor T cells within the liver. These findings show a general approach to focus systemic cancer immunotherapies to specific organs bearing tumor metastases by taking advantage of differential tropisms and the proinflammatory nature of microbes. (Cancer Res 2006; 66(2): 1096-104)

Introduction

There are three requirements for a therapeutically effective immune response against systemic cancer. First, a sufficient number of tumor-specific lymphocytes must be generated within the host. Second, these lymphocytes must traffic to sites of metastases. Third, the lymphocytes at the tumor site must execute the appropriate effector functions to destroy the cancer cells. Although significant numbers of circulating T cells capable of recognizing cancer antigens can be generated with various vaccination strategies or adoptive transfer of tumor-specific lymphocytes grown *ex vivo*, this typically does not result in tumor regression, particularly in the setting of bulky disease (1–10). Failure of these cells to efficiently home to sites of tumor metastases is becoming appreciated as an important limitation in this setting.

In this report, we explore a novel strategy to enhance the homing and activity of tumor-specific T cells into tumor deposits by administering a microbe that selectively targets an organ affected by metastases. We chose hepatic metastases for this proof-of-concept because the liver is one of the most important and often the sole site of metastatic cancer. This is particularly true for gastrointestinal cancers. For example, the majority of patients with advanced colorectal cancer will have metastatic disease limited only to the liver during some period of their illness, and one third of patients dying of colorectal cancer have metastatic disease limited to the liver on autopsy (11). Less than 20% of these patients with isolated hepatic metastases will have disease resectable for potential cure (12). Of the patients who undergo complete resection, ~30% to 40% of these patients will survive 5 years and half will be with evidence of disease.

As a means of regulating the inflammatory milieu of the liver, we have used engineered attenuated strains of *Listeria monocytogenes*, a bacterium that preferentially infects the liver. When administered by any of several routes, *L. monocytogenes* will initially be found in many organs but concentrates into the liver where they infect the hepatocytes and Kupffer cells and less so into the spleen (13, 14). This process results in a transient hepatitis associated with the induction of multiple proinflammatory cytokines and chemokines. We reasoned that this proinflammatory milieu could enhance the trafficking and activity of T cells within the liver. Using a model of hepatic metastases of colorectal cancer, we show that administration of *L. monocytogenes* significantly enhances the antitumor activity of a cancer vaccine. This enhanced activity is not observed for metastases in the lung. The immunologic mechanisms for this liver-specific effect result from both increased intrahepatic innate immunity and enhanced activity of tumor-specific T cells.

Materials and Methods

Animals and tumor cell lines. BALB/c mice (8-10 weeks old, female) were purchased from the National Cancer Institute. Colon tumor CT26 cells are murine colon adenocarcinoma cells derived from BALB/c mice (15). GVAX are CT26 cells transduced with the cDNA of granulocyte-macrophage colony-stimulating factor (GM-CSF) via a retroviral vector (16). These cell lines were maintained in RPMI 1640 supplemented with 10% heat-inactivated FCS (HyClone, South Logan, UT), 1 mmol/L sodium pyruvate, 2 mmol/L L-glutamine, nonessential amino acids (1% of 100× stock), 25 mmol/L HEPES buffer, and 50 μmol/L 2-mercaptoethanol (C-Media). The murine macrophage cell line J774 was purchased from American Type Culture Collection (Rockville, MD). All experimental subjects were treated ethically in accordance with a protocol approved by the Johns Hopkins Animal Care and Use Committee and in compliance with the Animal Welfare Act.

Note: K. Yoshimura and A. Jain contributed equally to this work.

Supplementary data for this article are available at Cancer Research Online (http://cancerres.aacrjournals.org/).

Requests for reprints: Richard D. Schulick, Department of Surgery and Oncology, Johns Hopkins Medical Institutions, The Bunting-Blaustein Cancer Research Building, Suite 442, 1650 Orleans Street, Baltimore, MD 21231. Phone: 410-614-9879; Fax: 410-614-9882; E-mail: rschulick@jhmi.edu.

doi:10.1158/0008-5472.CAN-05-2307

***L. monocytogenes* strains.** *L. monocytogenes* mutant strains used in this study were kind gifts from Daniel Portnoy (University of California, Berkeley, Berkeley, CA). The creation of these strains has been described previously. *L. monocytogenes*-actA (LM-actA) and *L. monocytogenes*-listeriolysin-O (LM-LLO) were each derived from wild-type *L. monocytogenes* (LM-Wild) and contain in-frame deletions in the *actA* and *hly* genes, respectively (17–20). The attenuated phenotypes of LM-actA and LM-LLO, respectively, result from defective cell-to-cell spread and inability to escape from the phagolysosome of infected cells. *L. monocytogenes*-L461T (LM-L461T) was derived from LM-Wild and has a cytotoxic phenotype through expression of a pH-insensitive LLO protein (L461T) engineered by site-directed mutation of *hly* (Fig. 1*C*; ref. 19). All *Lm* attenuated mutant strains were grown in brain-heart infusion (BHI) medium (Difco Laboratories). Bacteria for animal studies were harvested at mid-log phase of growth, purified by standard methods, formulated in PBS/8% DMSO at a concentration of $\sim 1 \times 10^{10}$ colony-forming units (CFU)/mL, and stored at −80°C. For injection, bacteria were thawed on ice and diluted in PBS according to injection doses in a volume of 100 μL corresponding to 0.1 median lethality ($0.1 \times LD_{50}$) in BALB/c mice as described (21).

Murine hepatic and pulmonary metastasis model. Mice were given isolated hepatic metastases using a hemispleen injection technique (22). Briefly, the spleens of anesthetized mice are divided into two halves and the halves are clipped. CT26 cells (1×10^5) are injected into one hemispleen, and after 30 seconds, that hemispleen is resected and the splenic vein draining the resected hemispleen is clipped. Mice were given isolated pulmonary metastases by tail vein injection of 1×10^5 CT26 cells suspended in 200 μL PBS using a 27-guage needle. In the experiment in which surface tumor nodules were counted in the liver, the mice from the various groups were sacrificed on day 17 and surface nodules were manually counted.

Treatment of mice with GVAX vaccine and *L. monocytogenes* in tumor model. A vaccination with GVAX consisted of 1×10^6 irradiated (5,000 rad) cells secreting 400 ng GM-CSF per 24 hours per 1×10^6 cells. Each vaccination consisted of a total dose of 1×10^6 cells in 300 μL PBS divided into three s.c. injections in three separate limbs. Mice that received GVAX vaccination were treated on day 3 after tumor challenge and then on days 6, 13, and 20 if not sacrificed prior. Mice that received LM-actA treatment received a single i.p. injection of $0.1 \times LD_{50}$ (1×10^7 CFU) as described above on day 6 after tumor challenge (21).

Rechallenge of mice for *in vivo* assessment of memory response. Mice were challenged with hepatic metastases and treated with LM-actA and GVAX. Sixty days after tumor injection, the surviving mice and naive BALB/c mice were rechallenged s.c. with 2×10^5 CT26 cells suspended in 100 μL PBS using a 27-guage needle into the right abdominal wall. Tumor volumes were measured in mm^3 with calipers and calculated with the following formula: $a \times b^2 / 2$, where a is the larger and b is the smaller of the two dimensions.

Infection of CT26 or J774 cells by LM-actA. CT26 or J774 cells ($\sim 2 \times 10^5$) were plated per well of a 24-well dish and incubated with *L. monocytogenes* at different multiplicity of infection (MOI) for 1 hour in serum-free, antibiotic-free medium. They were then incubated with gentamicin (50 μg/mL) for 1 hour. Cells were lysed with sterile water and plated on BHI plates. Percent infection was calculated by the formula: (number of bacteria after infection) / (bacterial input).

Treatment of mice with *L. monocytogenes* to determine CFU, natural killer, and natural killer T-cell infiltration in liver and spleen. To determine CFU in the liver and spleen of mice, 10^7 CFU of LM-actA were given i.v. to mice, and three mice per group per time point were sacrificed. The livers and spleens were minced and the CFU were determined by incubating serial dilutions on BHI plates.

To determine the percentage of natural killer (NK) and NK T cells present in the liver and spleen as a percentage of total leukocytes, these organs were harvested 1 day after various doses of LM-actA were given i.v. ranging from

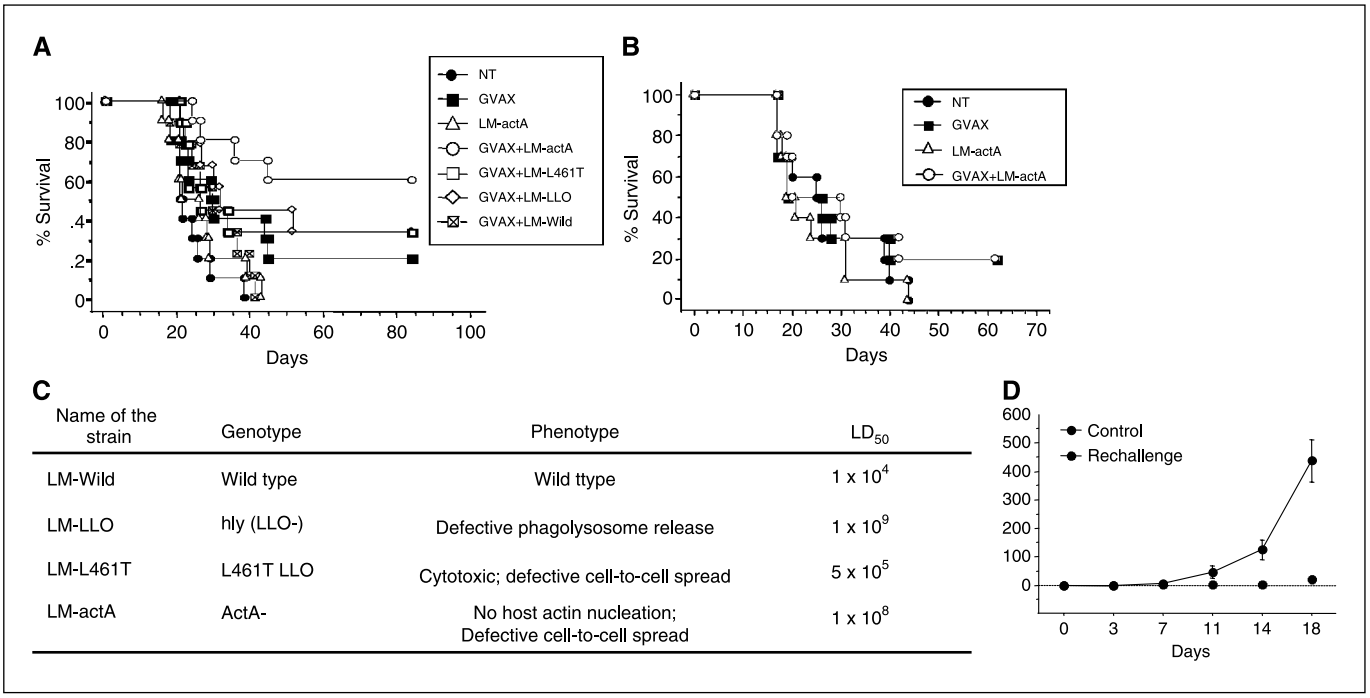

Name of the strain	Genotype	Phenotype	LD_{50}
LM-Wild	Wild type	Wild ttype	1×10^4
LM-LLO	hly (LLO-)	Defective phagolysosome release	1×10^9
LM-L461T	L461T LLO	Cytotoxic; defective cell-to-cell spread	5×10^5
LM-actA	ActA-	No host actin nucleation; Defective cell-to-cell spread	1×10^8

Figure 1. Synergy between tumor vaccine and various *Listeria* strains in the treatment of hepatic metastases. Survival curves of mice bearing hepatic metastases (*A*) or pulmonary metastases (*B*) of CT26 tumor and left untreated (*NT*), treated with GVAX alone, actA attenuated *L. monocytogenes* alone (LM-actA), or GVAX in combination with one of the *L. monocytogenes* strains. The *L. monocytogenes* strains used in combination with the GVAX were wild-type (LM-Wild) or one of the attenuated strains (LM-actA, LM-L461T, or LM-LLO). Mice that received GVAX vaccination were treated on day 3 after tumor challenge and then on days 6, 13, and 20. Treatment with the various *Listeria* strains was with a single i.p. injection of $0.1 \times LD_{50}$ on day 6 after tumor challenge. *A,* in mice challenged with hepatic metastases, the combination of GVAX with LM-actA resulted in a significant improvement in survival. $P < 0.01$ GVAX + LM-actA versus NT, $P < 0.05$ GVAX + LM-actA versus GVAX. *B,* in mice challenged with pulmonary metastases, there was no synergism with the LM-actA strain. *C,* table comparing the genotype, phenotype, and LD_{50} of the three attenuated strains and wild-type of *L. monocytogenes* used in these experiments. *D,* mice that were challenged with hepatic metastases, treated with GVAX + LM-actA, and survived long-term were rechallenged with a flank s.c. injection. In contrast to naive mice, they had minimal to no tumor growth.

0.01 to 0.25 × LD_{50} (LD_{50} = 10^8 CFU). NK and NK T cells were calculated in the livers using the protocol described below. These cell populations in the spleen were calculated by simply mashing the spleens, lysing the RBC, and staining by flow cytometry.

Isolation and analysis of liver-infiltrating lymphocytes. For analysis of NK, NK T, $CD4^+$, and $CD8^+$ T cells, three livers were processed per group and pooled. Each liver was mashed through a 100-μm nylon mesh filter into a 50 mL cone and brought to a volume of 45 to 50 mL medium. This suspension was spun at 1,500 rpm for 10 minutes at 4°C. The supernatant was aspirated and cell pellets were resuspended in 5 mL of 100% Percoll, 10 mL RPMI 1640, and 2 to 3 drops of heparin, vortexed, and centrifuged at room temperature for 20 minutes continuously. Supernatants were aspirated. Pellets were resuspended in 5 mL C-Media. One fifth of the cells were removed for flow cytometry to delineate the different cell populations.

For analysis of AH-1-specific $CD8^+$ T cells, the remaining four fifth of the cells were then enriched for $CD8^+$ T cells using a magnetic $CD8^+$ T-cell isolation protocol (MACS, Miltenyi Biotec, Auburn, CA). After magnetic enrichment, cells were resuspended in PBS supplemented with 0.5 mmol/L EDTA and 1% heat-inactivated FCS [fluorescence-activated cell sorting (FACS) buffer]. These cells were then assayed for presence of AH1-specific T-cell receptors as described below.

For isolation and assay of dendritic cells, two livers per group were cut into small pieces in C-Media. Liberase Blendzyme 2 (400 units/100 μL; Roche) and 1 mL of 0.1% DNase I (Roche) were added and mixed gently. After 30 minutes, EDTA (100 mmol/L) was added. After 5 minutes, cells were passed via strainer and remaining pieces were smashed through. After centrifuging at 1,500 rpm, cells were resuspended and an Accu-Paque Mammalian Lymphocyte Separation Protocol (Accurate Chemicals) was used. After washing, pellets were resuspended with FACS buffer.

Cell staining and flow cytometry. Following the isolation of liver-infiltrating immune cell populations from the mouse livers, cells were stained with CD4-FITC (Caltag), B220-FITC (PharMingen), CD8-CyChrome (PharMingen), CD3-FITC (PharMingen), DX5-phycoerythrin (PE; PharMingen), and CD11c-PE (PharMingen) and assayed on a FACScan flow cytometer (Becton Dickinson). Analysis of AH1 tumor-specific CD8 T cells was done using Ld-AH1 tetramer loaded with either AH1 (SPSYVYHQF) or the negative control β-galactosidase (TPHPARIGL) provided by the NIH Core Facility.

Quantitative real-time PCR analysis of liver-infiltrating cell populations for IFN-γ. AH1-specific $CD8^+$ T cells or NK cells were isolated as described above and immediately used for RNA extraction using Trizol reagent (Invitrogen). Reverse transcription was done with the SuperScript II First-Strand Synthesis System (Invitrogen). cDNA levels were analyzed by quantitative real-time PCR with the Taqman system (Applied Biosystems). Each sample was assayed in duplicates for the target gene together with 18S rRNA as the internal reference in 25 mL final reaction volume using the Taqman Universal PCR Master Mix and the ABI Prism 7700 Sequence Detection System. Premade reaction reagents were purchased from Applied Biosystems for detection of IFN-γ. The relative mRNA frequencies were determined by normalization to the internal control 18S RNA.

***In vivo* depletion of $CD4^+$, $CD8^+$ T, NK, and NK T cells.** To deplete NK cells, mice were given i.p. injections of 100 μL anti-asialo-GM1 antibody (Waco Chemicals) or HBSS (Life Technologies) on 7 and 4 days before the tumor challenge and 6 days after tumor challenge and then once weekly until death. To deplete $CD4^+$ or $CD8^+$ T cells, mice were injected with 250 μg mouse monoclonal antibodies against $CD4^+$ T cells (GK 1.5) or $CD8^+$ T cells (2.43; Lofstrand Labs Ltd.) or HBSS only (control) on 8, 4, and 1 days before the tumor challenge and 6 days after tumor challenge and then once weekly. Flow cytometric analysis was done verifying 99% depletion of $CD4^+$ and $CD8^+$ T-cell subsets as well as 81% of NK cell subset in the spleen after the administration of depleting antibodies (data not shown).

Histologic evaluation. On days 7, 9, 13, and 17 after tumor challenge (days 1, 3, 7, and 11 after *L. monocytogenes*), livers were dissected, fixed in 10% neutral buffered formalin, and embedded in paraffin. Sections (4 μm) were stained with H&E.

Statistical analysis. Statistical analyses were done by log-rank test for survival and *t* tests for tumor volume and nodules studies. $P = 0.05$ was considered statistically significant.

Results

***L. monocytogenes* enhances the antitumor activity of a vaccine against hepatic metastases.** To evaluate the capacity of *L. monocytogenes* to target vaccine-induced immune responses to the liver, we used a hepatic metastasis model of the BALB/c-derived colon tumor CT26 in which the spleen is surgically divided, cells are injected into one of the hemispleens, and that hemispleen is removed before closure (22). This results in isolated hepatic metastases while leaving the mouse functionally eusplenic. As a vaccine, we administered irradiated GM-CSF-transfected CT26 cells (GVAX) s.c., which have been well characterized and generated CD8 responses against an immunodominant H-$2L^d$-restricted, gp70-derived epitope termed AH1 (16, 23). GVAX is very effective at protecting mice from subsequent challenge with live tumor cells but has quite limited activity against CT26 tumors established even as soon as 3 days before vaccination. As shown in Fig. 1*A*, GVAX has relatively little effect on the overall mortality of mice with 3-day established hepatic metastases, although 20% of vaccinated mice commonly survive long-term. These findings are highly reproducible among 10 separate experiments.

We initially evaluated the capacity of several mutant *L. monocytogenes* strains to enhance liver targeting of antitumor immunity and compared them with the wild-type strain. Three highly virulence-attenuated mutants were used in these studies. Listeriolysin-O-deleted strains (LM-LLO) fail to produce the *Listeria* hemolysin necessary for transfer of *L. monocytogenes* out of the phagolysosome and into the cytosol (18, 20). A second *L. monocytogenes* strain whose LLO gene contains a point mutation (*L. monocytogenes*-L416T) produces a non-pH-dependent listeriolysin that is lethal to infected cells, thereby aborting the *Listeria* life cycle (19, 24). Finally, an actA-deleted strain (LM-actA) fails to produce the actA protein necessary for induction of polymerization of cytosolic actin filaments necessary for cell-to-cell spread of *L. monocytogenes* (17). Therefore, actA mutants can only infect a single cell *in vivo*. As shown in Fig. 1*C*, all of these mutant *L. monocytogenes* strains are highly attenuated (between 10^3- and 10^5-fold) relative to LM-Wild, which has a LD_{50} of 1×10^4 in BALB/c mice. In evaluating the capacity of the different *L. monocytogenes* mutants to enhance hepatic targeting of GVAX-induced antitumor immune responses, we normalized for potential differences in bacterial load by using 0.1 × LD_{50} of each strain. Figure 1*A* shows that, although each of the attenuated strains resulted in enhanced survival of mice bearing hepatic metastases of CT26 when combined with GVAX, the LM-actA mutant provided the greatest survival advantage in comparison with untreated mice ($P < 0.01$) and mice treated with GVAX alone ($P < 0.05$). This mutant strain has therefore been chosen for subsequent development and analysis of immunologic mechanisms. Of note, when LM-actA was used alone or when LM-Wild was used in combination with GVAX, there was no augmentation in survival. The increase in the LD_{50} of the attenuated strains allowed these bacteria to be given at much higher concentration effectively greatly increasing their therapeutic window. The hepatotropism of each of the attenuated

strains relative to wild-type has not been altered. Figure 1*B* shows that LM-actA does not enhance GVAX-induced antitumor responses against lung metastases from CT26. Therefore, the hepatic-specific targeting of antitumor responses is observed for multiple *L. monocytogenes* strains, each of which selectively infects the liver *in vivo*.

Six mice that had survived beyond 60 days after hepatic tumor challenge and treatment with GVAX plus LM-actA were then rechallenged with s.c. tumor as described. Five of the six mice did not have any tumor growth and one had minimal tumor growth, whereas all of the naive mice ($n = 5$) had vigorous tumor growth (Fig. 1*D*). This was highly statistically significant at both 14 and 18 days ($P < 0.005$ for both).

Intrahepatic cellular responses induced by LM-actA administration. As a prelude to evaluating whether the liver-specific antitumor responses induced by the combination of GVAX and *Listeria* are in part due to direct infection of tumor cells by the bacterium, an *in vitro* infection assay was done in which the bacteria were cocultured with CT26 and J774 (a murine macrophage cell line) at different MOI ratios (Fig. 2*A*). Whereas the control J774 cells were efficiently infected, CT-26 cells are essentially not infected (<0.01% at all MOI; Fig. 2*A*).

As described above, *L. monocytogenes* has a strong tropism for the liver but is also found at significant levels in the spleen after infection. Figure 2*B* shows that, after i.v. injection of LM-actA, many CFU can be isolated from both the liver and the spleen, although the duration of this infection is longer in the liver. Despite this, a significant innate immune response characterized by a large influx of NK and NK T cells can only be found in the liver (Fig. 2*C* and *D*). Not only is there a failure of expansion of NK and NK T-cell populations in the spleen after LM-actA infection, there is actually a ~50% decrease in the numbers of these cells in the spleen, compatible with a redistribution into the liver.

The finding that LM-actA infection does not by itself enhance survival of mice bearing hepatic metastases of CT26 but rather enhances the antitumor effects when used in conjunction with a GVAX vaccine suggests that an important function of LM-actA is to enhance the trafficking and/or activity of vaccine-induced tumor antigen-specific T cells in the liver. However, it is equally possible that *L. monocytogenes* infection activates local innate effectors within the hepatic environment that in turn can act in concert with vaccine-induced antitumor effectors. The most direct initial approach to dissecting immunologic mechanisms of hepatic

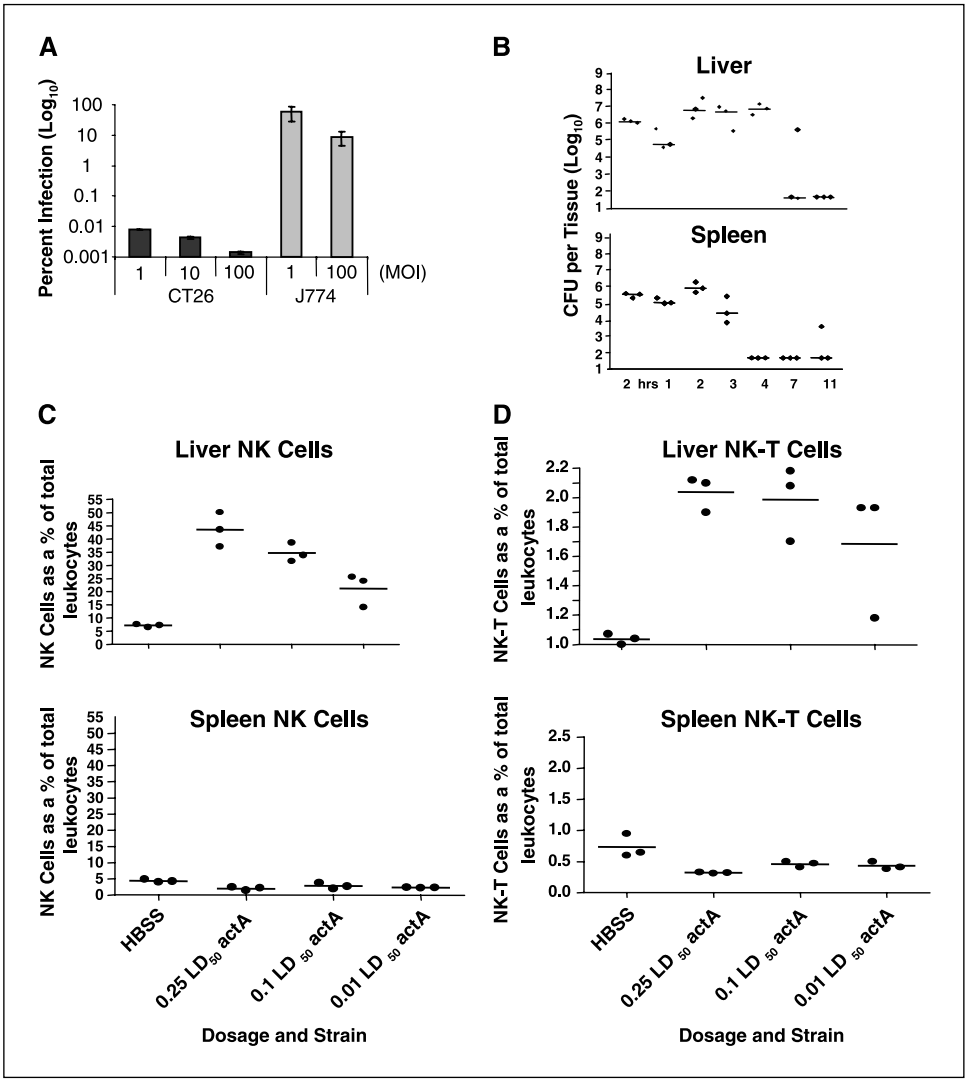

Figure 2. *Listeria* does not directly infect CT26 tumor cells and selectively induces innate immune activation within the liver. *A, Listeria* were cocultured with CT26 and J774 (a murine macrophage cell line) at different MOI ratios. The control J774 cells were efficiently infected, whereas CT26 cells were essentially not infected (<0.01% at all MOI). *B,* mice were injected with 1×10^7 CFU of LM-actA i.v. At the indicated time points, spleen and livers were harvested and CFU were enumerated. LM-actA can be isolated from both the liver and the spleen in significant amounts after infection. *C* and *D,* 48 hours after infection with LM-actA, NK and NK T cells within the liver and spleen were enumerated.

targeting of LM-actA is to examine leukocyte populations that infiltrate into or expand within the liver. Livers from mice treated with either GVAX alone, LM-actA alone, both, or neither were harvested at various time points after tumor challenge. After a collagenase digestion procedure, intrahepatic cell populations were delineated by flow cytometry (Supplementary Data 1). There was a dramatic increase in virtually all cell types examined, including NK cells, NK T cells, plasmacytoid dendritic cells, myeloid dendritic cells, and T cells. Not surprisingly, innate effectors, including NK cells, NK T cells, and plasmacytoid dendritic cells, were significantly increased in all groups receiving LM-actA (Fig. 3*A* and *C-E*). The expansion in these innate effectors occurred relatively quickly (3 days after LM-actA). In contrast, the increase in T-cell numbers (primarily $CD8^+$ T cells) peaked somewhat later (7 days after LM-actA; Fig. 3*B*). Interestingly, treatment with both vaccine and LM-actA resulted in the most pronounced increase in $CD8^+$ T-cell infiltration into the liver peaking on day 13 after tumor challenge (day 7 after LM-actA and day 10 after GVAX). Infiltration of plasmacytoid dendritic cells occurred somewhat earlier than myeloid dendritic cells and both were dependent on administration of LM-actA.

Tumor-specific T-cell responses and NK activation in tumor-bearing livers as a result of LM-actA administration. The identification of an immunodominant MHC class I (Ld-AH1)–restricted antigenic target from CT26 (termed AH1 and derived from an endogenous retroviral *env* gene product) allowed us to use Ld-AH1 tetramers to directly assess the numbers of AH1-specific T cells within the liver. Although significant numbers of AH1-specific T cells could be detected in tumor-bearing livers from mice under all treatment conditions, a greater proportion of AH1-specific T cells were identified in animals vaccinated with GVAX and particularly with a combination of GVAX and LM-actA. Calculation of total number of AH1-specific $CD8^+$ cells in the liver has shown that this tumor-specific T-cell population peaked at day 13, the same time that the total $CD8^+$ T-cell population peaked. Significantly, a much greater peak level of AH1-specific $CD8^+$ T cells was observed in animals receiving both GVAX and LM-actA relative to all other treatment groups (Fig. 4). Concomitant with the increase in AH1-specific $CD8^+$ T cells in livers of animals treated with GVAX and LM-actA, there is a dramatic decrease in AH1-specific $CD8^+$ T cells in the spleen (similar to what was observed with the innate response; Fig. 2), compatible with a redistribution of tumor-specific T cells into the liver induced by the *L. monocytogenes* (Supplementary Data 2).

To investigate the activation state of both tumor-specific $CD8^+$ T cells and NK cells within the liver, we challenged mice with hepatic metastases and then left them untreated or treated with GVAX, LM-actA, or both. Mice were sacrificed on days 7, 9, 13, and 17 after tumor challenge (days 1, 3, 7, and 10 after LM-actA infection) and liver-infiltrating lymphocytes were isolated. In addition, Ld-AH1 $tetramer^+$ $CD8^+$ T cells and NK cells were sorted and RNA was prepared from these cells. Expression of IFN-γ mRNA was then measured using quantitative PCR. Tumor-specific $CD8^+$ T cells isolated from livers of mice treated with both GVAX and LM-actA had higher levels of IFN-γ RNA expression, indicating that they were more highly activated. This increased level of IFN-γ mRNA relative to other groups was present at 13 days after tumor challenge or 7 days after LM-actA treatment. Taken together with total numbers of AH1-specific cells, these results show that the combination of GVAX together with administration of LM-actA significantly increased both the number and the activation state of tumor-specific T cells within the liver. Interestingly, NK cells isolated from livers of mice treated with both GVAX and LM-actA had the highest levels of IFN-γ RNA expression, although this increased level occurred

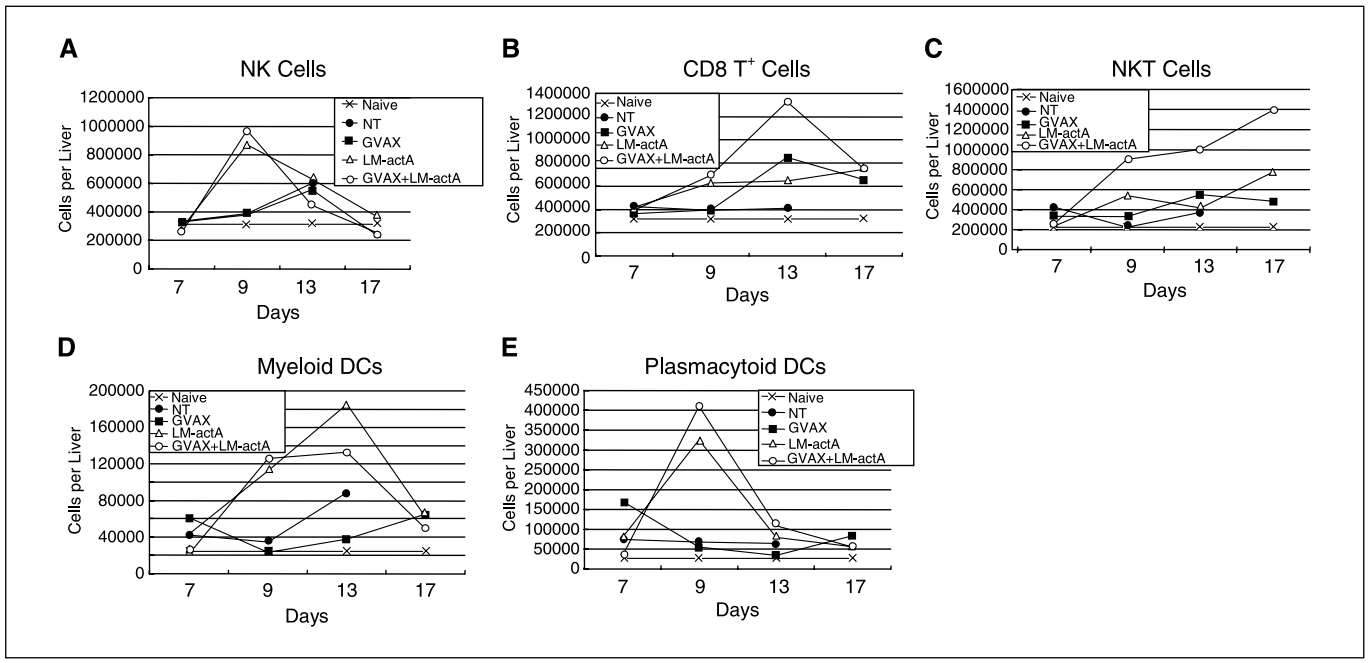

Figure 3. Kinetics of liver-infiltrating cell populations in mice bearing hepatic metastases. Mice bearing hepatic metastases of CT26 were left untreated or treated with GVAX, LM-actA, or both as in Fig. 1. Naive tumor-free mice were also analyzed. Livers from each group were harvested at four time points, 7, 9, 13, and 17 days after tumor challenge, and processed for flow cytometry analysis. Total cells/liver were enumerated at different time points for NK cells (*A*), $CD8^+$ T cells (*B*), NK T cells (*C*), myeloid dendritic cells (*DCs*; *D*), and plasmacytoid dendritic cells (*E*).

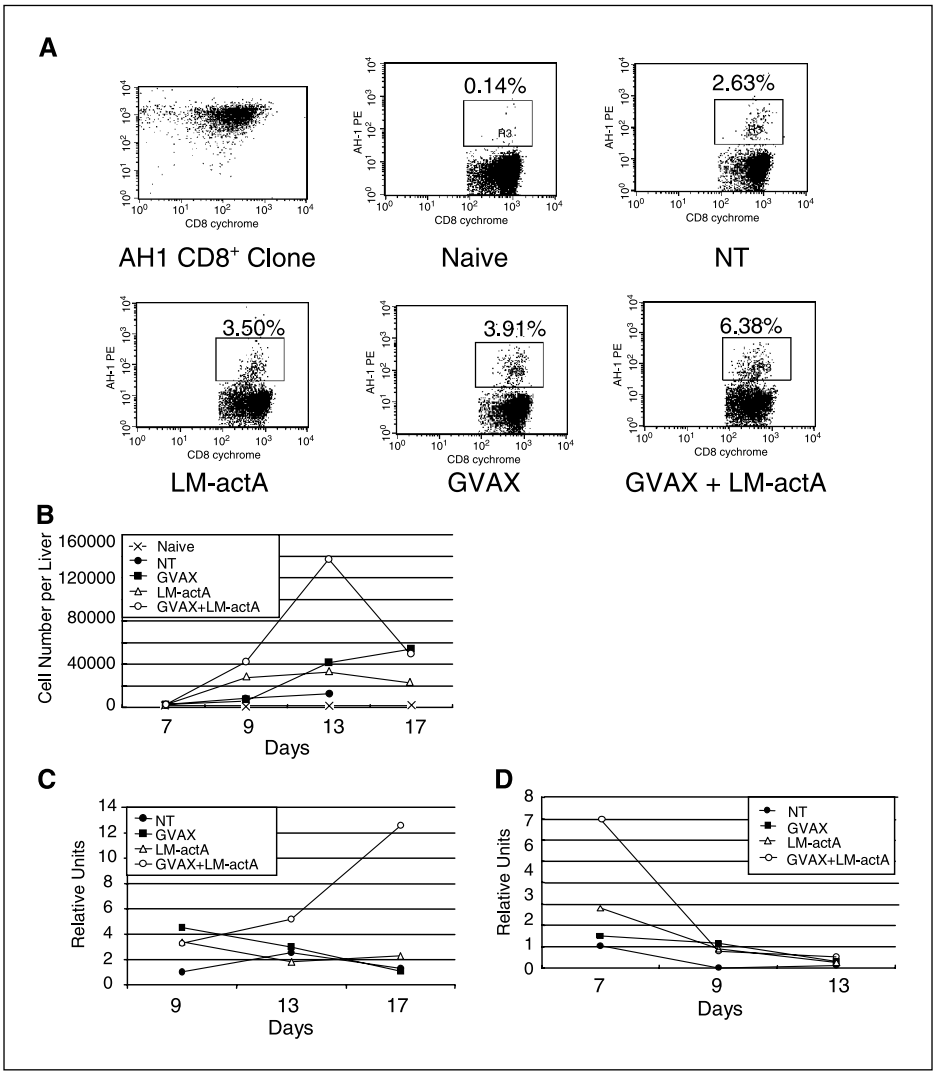

Figure 4. Analysis of tumor-specific CD8$^+$ T cells that infiltrate the liver in treated mice with hepatic metastases. Mice bearing hepatic metastases of CT26 were left untreated or treated with GVAX, LM-actA, or both as in Fig. 1. *A,* specific flow cytometry plots on cells isolated from the livers of mice sacrificed on day 13 and stained with anti-CD8 (*green*) and Ld-AH1 tetramers (*red*). AH1 is the immunodominant MHC class I–restricted tumor antigen recognized by CT26-specific CD8$^+$ T cells. Positive and negative controls are shown using an AH1-specific CD8$^+$ T-cell clone and hepatic CD8$^+$ cells from naive non-tumor-bearing mice. *B,* absolute number of AH1-specific CD8$^+$ T cells that infiltrate the liver at various time points. Treatment with both GVAX and LM-actA resulted in the highest numbers of tumor-specific CD8$^+$ T cells infiltrating the liver on day 13. *C,* AH1-specific CD8$^+$ T cells infiltrating the liver were sorted by flow cytometry and used to extract mRNA for quantitative PCR assays for IFN-γ. An equal number of Ld-AH1 tetramer$^+$ cells was used for each sample. Treatment with both GVAX and LM-actA resulted in the highest expression of IFN-γ mRNA/Ld-AH1 tetramer$^+$ cells. *D,* additionally, IFN-γ mRNA expression was similarly examined in sorter-purified hepatic NK cells and was found to be elevated in the group treated with both GVAX and LM-actA but at earlier time points.

earlier in the time course and was apparent 7 days after tumor challenge or 1 day after LM-actA treatment. The finding that NK activation state as measured by IFN-γ RNA is not exclusively dependent on LM-actA administration but is further enhanced in animals receiving the combination of GVAX vaccination and LM-actA suggests a cross-talk between the innate and the adaptive arms of the intrahepatic immune response. Although there was a significant expansion in the overall number of NK T cells, there was not a significant increase in IFN-γ mRNA expression by this population (data not shown).

Although increases in cell number and activation state suggest a potential role for a lymphocyte subset in the antitumor response, definitive evidence involves the demonstration that depletion of that subset abrogates the antitumor response. Therefore, tumor-bearing mice treated with the GVAX plus LM-actA combination were treated with depleting antibodies before challenging mice with tumor in the hepatic metastasis model. As in the earlier studies, control mice treated with GVAX and LM-actA showed a 50% long-term survival rate. However, the GVAX plus LM-actA therapy completely failed to treat animals depleted of either NK cells or CD8$^+$ T cells (Fig. 5). These results confirm that these two lymphocyte populations are critical for mediating the intrahepatic antitumor response. When given wild-type or less attenuated strains of *L. monocytogenes*, NK-depleted animals died of *L. monocytogenes* infection alone, further proving the relative safety of LM-actA (data not shown). Taken together with the studies in Figs. 3 and 4, they show an important collaboration between local innate effectors and antigen-specific CD8$^+$ T cells in mediating a successful intrahepatic antitumor response. In contrast, mice depleted of CD4$^+$ T cells seemed to respond to the GVAX plus LM-actA treatment equivalently to control animals. This result does not absolutely eliminate a role of CD4$^+$ T cells because it is now appreciated that the CD4$^+$ subset contains both helper T cells and regulatory T cells. It is therefore possible that depletion of total CD4$^+$ T cells resulted in offsetting responses from elimination of both T helper and regulatory T cells. Further dissection of the relative roles of CD4$^+$ T-cell subsets (i.e., helper and regulatory) will require additional evaluation.

In addition to defining the relevant lymphocyte subsets involved in the antitumor response against hepatic metastases, we investigated the patterns of liver infiltration by lymphocytes after tumor challenge in the various treatments. On day 17 after tumor challenge, livers were removed and surface nodules were counted. Each group had five mice. The no treatment group had the highest

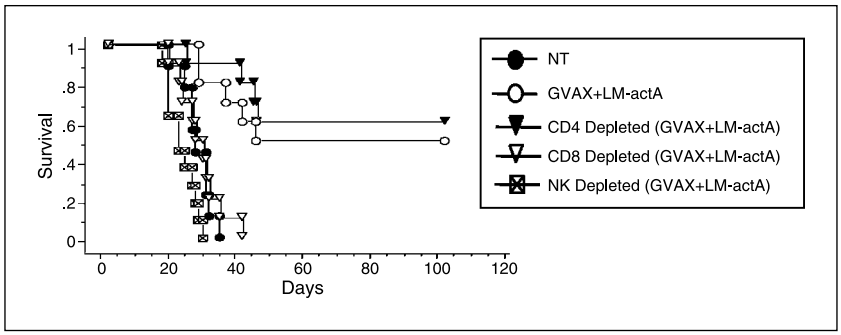

Figure 5. Depletion of specific cell populations in mice challenged with hepatic metastases and then treated with both GVAX and LM-actA. Mice bearing hepatic metastases and treated with GVAX + LM-actA were left intact or depleted *in vivo* of $CD4^+$ T cells using GK1.5 antibody, $CD8^+$ cells using 2.43 antibody, or NK cells using asialo-GM1 antibody (at doses that did not deplete NK T cells). Depletion of >90% was confirmed by flow cytometry analysis of liver and spleen from one to two animals in each group. Survival of animals was followed. All nonsurviving animals were found to possess significant amounts of hepatic tumor. There was no mortality in subset-depleted non-tumor-bearing animals treated with GVAX + LM-actA (data not shown).

number of nodules (8-17), the GVAX group had 2 to 5 nodules, the LM-actA group had 6 to 7 nodules, and the combination therapy group had 0 to 1 nodule. There was a highly significant difference between the number of nodules seen in the combination group compared with the other groups ($P < 0.001$; Fig. 6*A*).

Mice were also sacrificed at 13 days after tumor challenge (7 days after *L. monocytogenes* treatment) and the livers were subjected to H&E staining (Fig. 6*B*). Mice that were untreated after hepatic tumor challenge had large fields of visible tumor with relatively little lymphocyte infiltration into the tumor. Mice that were treated with GVAX alone showed some tumor infiltration by lymphocytes but little infiltration into the hepatic parenchyma. Disease volume in these mice was less than in the untreated mice, indicating that GVAX vaccines alone indeed generated a partially effective immune response capable of accessing hepatic metastases, but which in the majority of cases was insufficient to eliminate tumors. Mice that were treated with LM-actA alone also had somewhat decreased disease volume, but the pattern of lymphocyte infiltration was more diffuse throughout the hepatic parenchyma. Mice that were treated with both GVAX and LM-actA had either no disease evident or very small volume of disease on day 13. These livers tended to exhibit foci of lymphocyte infiltrates, which may be associated with tumor deposits that had been successfully killed before the histologic evaluation on day 13 (Fig. 6*B*).

Discussion

We have used an engineered live-attenuated *L. monocytogenes*, which preferentially homes to the liver following systemic administration, to target antitumor immune responses into the liver for the treatment of hepatic metastases. We show that this immunorecruitment approach synergizes with a tumor vaccine that provides very weak antitumor responses on its own. The mechanism of action seems to involve at least three elements: increased activation of local innate effectors (i.e., NK cells), increased numbers of tumor-specific T cells that enter and/or expand within the liver, and increased activity of these cells. There is no enhanced activity of the tumor vaccine against lung metastases.

L. monocytogenes is a ubiquitous Gram-positive facultative intracellular bacterium that has been studied for four decades as a model for stimulating both innate and T-cell-dependent antibacterial immunity. The ability of *L. monocytogenes* to effectively stimulate cellular immunity is based on its intracellular lifecycle (25). On infecting the host, the bacterium is rapidly taken up by phagocytes into a phagolysosomal compartment. The bacterium is hepatotrophic and is efficiently phagocytosed by Kupffer cells and other phagocytes within the liver. Furthermore, internalin B is a *L. monocytogenes* protein that promotes entry of the bacterium into certain mammalian cells by binding hepatocyte growth factor receptor (or c-met). Therefore, the primary site of infection by this bacterium is the liver. The majority of the bacteria are subsequently degraded, and the processed antigens are expressed on the surface of the antigen-presenting cells via the class II endosomal pathway. Within the acidic phagolysosome, certain bacterial genes are activated, including the cholesterol-dependent cytolysin, LLO, which can degrade the phagolysosome,

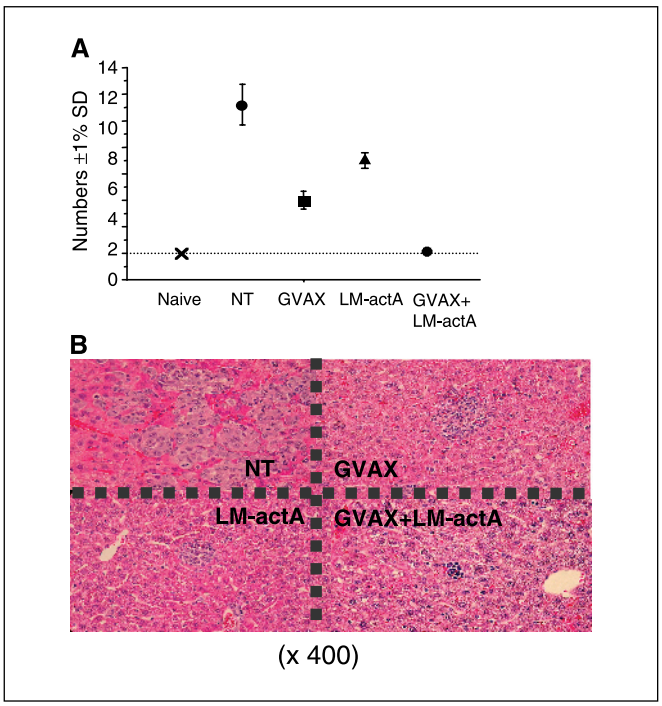

Figure 6. Liver nodules and histology of tumor-bearing mice treated with GVAX and LM-actA. *A,* mice were sacrificed 17 days after tumor challenge and surface nodules on the liver were counted after various treatments. Untreated mice had the most number of nodules followed by the LM-actA alone group and then the GVAX alone group, and the GVAX + LM-actA had no surface nodules. *B,* representative H&E staining of livers from mice that were challenged with hepatic metastases and were either untreated or treated with GVAX, LM-actA, or both on day 13. Mice that were untreated had large tumor burdens with little lymphocyte infiltration. GVAX treatment decreased tumor burden and caused increased infiltration of lymphocytes into tumor. LM-actA treatment also decreased tumor burden but caused a more diffuse pattern of lymphocyte infiltration into the liver. Treatment with both markedly decreased tumor burden (most mice without evidence of disease) and resulted in a diffuse pattern of lymphocyte infiltration into the liver but also specific pockets of lymphocyte infiltration.

releasing viable bacteria into the cytosolic compartment of the host cell. Surviving *L. monocytogenes* are able to divide and express gene products that are processed via the class I pathway, leading to the stimulation of $CD8^+$ T cells.

It is important to note that *L. monocytogenes* has been used as a vector for heterologous antigens and has been shown to induce regression of established syngeneic tumors in mouse models following systemic administration. For these reasons, *L. monocytogenes* is under active investigation as an antigen-specific vaccine vector for cancer and infectious disease (21, 26). The major focus of this work, however, is to exploit the ability of *L. monocytogenes* to target an immune response to the liver rather than its ability to generate an antigen-specific vaccine response by itself.

There is strong evidence that *L. monocytogenes* infection can focus an immune response into the liver. The host response against *L. monocytogenes* is characterized by a complex interplay between innate and adaptive immune elements (27). Dendritic cells, especially tumor necrosis factor-α and inducible nitric oxide synthase–producing dendritic cells, and NK cells producing IFN-γ play a crucial role in control of bacterial growth during the initial stage of the infection. $CD8^+$ T cells then are involved in the response and in the adaptive phase of the immune response. This interplay between the innate and the adaptive immune response occurs mostly within the liver as this is the primary site of infection.

Even stronger evidence comes from studies showing the importance of the microenvironment of the liver by Limmer et al. (28). Using a TCR-transgenic mouse system displaying peripheral tolerance against a liver-specific MHC class I Kb antigen, they investigated whether the breaking of tolerance would result in autoimmunity. Reversal of tolerance was attempted by simultaneous challenge with cells expressing the Kb autoantigen and interleukin-2 (IL-2). Tolerance could not be broken with IL-2 alone or when Kb- and IL-2-expressing cells were applied to different sites on the mice. However, despite the presence of activated autoreactive T cells that were able to reject Kb-positive grafts, no autoaggression against the Kb-positive liver was observed. These results indicate that breaking of tolerance is not sufficient to cause liver-specific autoimmunity. However, when in addition to breaking tolerance the mice were infected with a liver-specific pathogen, autoaggression occurred. Thus, in this system, at least two independent steps seem to be required for organ-specific autoimmunity: reversal of peripheral tolerance resulting in functional activation of autoreactive T cells and conditioning of the liver microenvironment that enabled the activated T cells to cause tissue damage.

In the studies presented, we have shown the ability of attenuated strains of *L. monocytogenes* to significantly augment the control of hepatic metastases in mice that were treated with GVAX. Additionally, this augmentation was organ specific and depended on the hepatotropism of the microorganism. The use of specifically attenuated strains of bacteria that targeted proteins involved in virulence without significantly altering the hepatotropism or immunogenicity allowed more efficient immune responses in the liver to eliminate hepatic metastases. When this strategy was used against pulmonary metastases, there was no augmentation. This was highly expected as the lung is not a significant site of infection for *L. monocytogenes*. This finding is similar to that found by Pan et al. (29). In their tumor model system, they used a B16 cell line engineered to express a foreign influenza virus antigen NP to increase its immunogenicity, and a recombinant *L. monocytogenes* strain that also expressed the same virus antigen. Thus, their strategy was to use a *L. monocytogenes* strain that infected mice and expressed a foreign antigen that stimulated the immune system to mount a response against that foreign antigen. Under the right conditions, they were able to stimulate the immune system of the mice to reject tumor cells in the lung. However, when they used a nontumor antigen-expressing *L. monocytogenes* strain, essentially all of the mice showed evidence of tumor nodules in the lung. It should be noted, however, that the nontumor antigen-expressing *L. monocytogenes* strain did cause some decrease in the number of nodules in the lung, although it did not totally eliminate disease.

A possible memory response was shown in the mice that were rechallenged with flank tumor after successfully eliminating hepatic disease following GVAX and LM-actA treatment.

The studies involving the kinetics of liver-infiltrating effector cells suggested that NK cells from the innate arm and $CD8^+$ T cells from the adaptive arm of the immune response were important for this response. This was further confirmed with depletion studies. Mice that were depleted of NK cells or $CD8^+$ T cells had abrogation of the combined treatment effect of GVAX and LM-actA. When mice were depleted of $CD4^+$ T cells, there was no abrogation of effect. It is likely that other cell types also play a role in this response. The kinetic studies also suggest liver infiltration by plasmacytoid dendritic cells followed by myeloid dendritic cells. The infiltration of these two subsets of dendritic cells is dependent on *L. monocytogenes* treatment and independent of GVAX treatment. We have also done studies using CD1d knockout mice that are deficient in NK T cells. There is no abrogation of response in these NK T-cell-deficient mice to the combined treatment of GVAX and LM-actA (data not shown).

The innate and adaptive immune response to *L. monocytogenes* within the liver seems to greatly augment the tumor-specific immune response through a bystander effect. We have shown that there is a strong early response with highly activated NK cells in response to *L. monocytogenes* treatment, which is independent of GVAX vaccination. This is followed by a strong response with highly activated tumor-specific $CD8^+$ T cells that requires both GVAX and *L. monocytogenes* treatment.

By histologic examination, GVAX vaccination caused increased lymphocyte infiltration into the tumor, whereas *L. monocytogenes* caused increased lymphocyte infiltration nonspecifically into the liver and tumor. Treatment with both caused a marked reduction of tumor with specific pockets of lymphocyte infiltrations.

In these experiments, we chose to use the BALB/c strain of mice and the CT26 cell line for several reasons, including (*a*) CT26 is a colorectal cancer line; (*b*) CT26 has an immunodominant antigen (AH1); (*c*) there are readily available reagents, such as the Ld-AH1 tetramer that allow tracking of the immune response; and (*d*) when injected into the hepatic metastasis model, isolated hepatic (and no lung) metastases are formed. We are currently developing a B16 melanoma cell line derived from the B6 murine background that also has a propensity for liver metastases. When available, we will also use this tumor model system as B6 mice tend to mount a more skewed Th1 response, whereas BALB/c mice tend to mount a more balanced Th1 and Th2 response (30–32). This may lead to differences in the degree of augmentation by *L. monocytogenes*.

In summary, we have shown a novel approach to use a tissue-specific bacterial infection to target an immune response against a tumor primed by a vaccine. In our model, we have taken advantage of the hepatotropism of *L. monocytogenes*. We have taken

advantage of the ability to segregate the virulence factors of *L. monocytogenes* from its ability to generate an immune response within the liver with specific and stable deletions of various proteins expressed by the organism. This has therapeutic potential in focusing a vaccine-primed immune response into the liver against gastrointestinal malignancies that have a high propensity to metastasize to the liver, such as colorectal, pancreatic, gastric, and esophageal cancers.

Acknowledgments

Received 7/1/2005; revised 10/13/2005; accepted 11/2/2005.

Grant support: NIH grant 1 K23 CA104160-01, Commonwealth Foundation, Charles Delmar Foundation, and gifts from Robert and Jacque Alvord, William and Betty Topercer, and Dorothy Needle.

The costs of publication of this article were defrayed in part by the payment of page charges. This article must therefore be hereby marked *advertisement* in accordance with 18 U.S.C. Section 1734 solely to indicate this fact.

We thank Daniel Portnoy, Ph.D., for providing reagents and helpful suggestions.

References

1. Liu M, Acres B, Balloul JM, et al. Gene-based vaccines and immunotherapeutics. Proc Natl Acad Sci U S A 2004;101 Suppl 2:14567–71.
2. Lewis JJ. Therapeutic cancer vaccines: using unique antigens. Proc Natl Acad Sci U S A 2004;101 Suppl 2:14653–6.
3. Stevenson FK, Ottensmeier CH, Johnson P, et al. DNA vaccines to attack cancer. Proc Natl Acad Sci U S A 2004; 101 Suppl 2:14646–52.
4. Blattman JN, Greenberg PD. Cancer immunotherapy: a treatment for the masses. Science 2004;305:200–5.
5. Berzofsky JA, Terabe M, Oh S, et al. Progress on new vaccine strategies for the immunotherapy and prevention of cancer. J Clin Invest 2004;113:1515–25.
6. Figdor CG, de Vries IJ, Lesterhuis WJ, Melief CJ. Dendritic cell immunotherapy: mapping the way. Nat Med 2004;10:475–80.
7. Gilboa E. The promise of cancer vaccines. Nat Rev Cancer 2004;4:401–11.
8. Rosenberg SA. Shedding light on immunotherapy for cancer. N Engl J Med 2004;350:1461–3.
9. Cerundolo V, Hermans IF, Salio M. Dendritic cells: a journey from laboratory to clinic. Nat Immunol 2004;5: 7–10.
10. Rosenberg SA, Yang JC, Restifo NP. Cancer immunotherapy: moving beyond current vaccines. Nat Med 2004;10:909–15.
11. Weiss L, Grundmann E, Torhorst J, et al. Haematogenous metastatic patterns in colonic carcinoma: an analysis of 1541 necropsies. J Pathol 1986; 150:195–203.
12. Sjovall A, Jarv V, Blomqvist L, et al. The potential for improved outcome in patients with hepatic metastases from colon cancer: a population-based study. Eur J Surg Oncol 2004;30:834–41.
13. Pope C, Kim SK, Marzo A, et al. Organ-specific regulation of the CD8 T cell response to *Listeria monocytogenes* infection. J Immunol 2001;166:3402–9.
14. Portnoy DA, Jacks PS, Hinrichs DJ. Role of hemolysin for the intracellular growth of *Listeria monocytogenes*. J Exp Med 1988;167:1459–71.
15. Corbett TH, Griswold DP, Jr., Roberts BJ, Peckham JC, Schabel FM, Jr. Tumor induction relationships in development of transplantable cancers of the colon in mice for chemotherapy assays, with a note on carcinogen structure. Cancer Res 1975;35:2434–9.
16. Dranoff G, Jaffee E, Lazenby A, et al. Vaccination with irradiated tumor cells engineered to secrete murine granulocyte-macrophage colony-stimulating factor stimulates potent, specific, and long-lasting anti-tumor immunity. Proc Natl Acad Sci U S A 1993;90:3539–43.
17. Skoble J, Portnoy DA, Welch MD. Three regions within ActA promote Arp2/3 complex-mediated actin nucleation and *Listeria monocytogenes* motility. J Cell Biol 2000;150:527–38.
18. Jones S, Portnoy DA. Characterization of *Listeria monocytogenes* pathogenesis in a strain expressing perfringolysin O in place of listeriolysin O. Infect Immun 1994;62:5608–13.
19. Glomski IJ, Gedde MM, Tsang AW, Swanson JA, Portnoy DA. The *Listeria monocytogenes* hemolysin has an acidic pH optimum to compartmentalize activity and prevent damage to infected host cells. J Cell Biol 2002; 156:1029–38.
20. Lauer P, Chow MY, Loessner MJ, Portnoy DA, Calender R. Construction, characterization, and use of two *Listeria monocytogenes* site-specific phage integration vectors. J Bacteriol 2002;184:4177–86.
21. Brockstedt DG, Giedlin MA, Leong ML, et al. *Listeria*-based cancer vaccines that segregate immunogenicity from toxicity. Proc Natl Acad Sci U S A 2004;101:13832–7.
22. Jain A, Slansky JE, Matey LC, Allen HE, Pardoll DM, Schulick RD. Synergistic effect of a granulocyte-macrophage colony-stimulating factor-transduced tumor vaccine and systemic interleukin-2 in the treatment of murine colorectal cancer hepatic metastases. Ann Surg Oncol 2003;10:810–20.
23. Huang AY, Gulden PH, Woods AS, et al. The immunodominant major histocompatibility complex class I-restricted antigen of a murine colon tumor derives from an endogenous retroviral gene product. Proc Natl Acad Sci U S A 1996;93:9730–5.
24. Glomski IJ, Decatur AL, Portnoy DA. *Listeria monocytogenes* mutants that fail to compartmentalize listerolysin O activity are cytotoxic, avirulent, and unable to evade host extracellular defenses. Infect Immun 2003;71:6754–65.
25. Portnoy DA, Auerbuch V, Glomski IJ. The cell biology of *Listeria monocytogenes* infection: the intersection of bacterial pathogenesis and cell-mediated immunity. J Cell Biol 2002;158:409–14.
26. Paterson Y, Johnson RS. Progress towards the use of *Listeria monocytogenes* as a live bacterial vaccine vector for the delivery of HIV antigens. Expert Rev Vaccines 2004;3:S119–34.
27. Lara-Tejero M, Pamer EG. T cell responses to *Listeria monocytogenes*. Curr Opin Microbiol 2004;7:45–50.
28. Limmer A, Sacher T, Alferink J, et al. Failure to induce organ-specific autoimmunity by breaking of tolerance: importance of the microenvironment. Eur J Immunol 1998;28:2395–406.
29. Pan ZK, Weiskirch LM, Paterson Y. Regression of established B16F10 melanoma with a recombinant *Listeria monocytogenes* vaccine. Cancer Res 1999;59: 5264–9.
30. Galbiati F, Rogge L, Adorini L. IL-12 receptor regulation in IL-12-deficient BALB/c and C57BL/6 mice. Eur J Immunol 2000;30:29–37.
31. Guery JC, Galbiati F, Smiroldo S, et al. Selective development of T helper (Th)2 cells induced by continuous administration of low dose soluble proteins to normal and β(2)-microglobulin-deficient BALB/c mice. J Exp Med 1996;183:485–97.
32. Hsieh CS, Macatonia SE, O'Garra A, et al. T cell genetic background determines default T helper phenotype development *in vitro*. J Exp Med 1995;181: 713–21.

Selective Targeting of Antitumor Immune Responses with Engineered Live-Attenuated *Listeria monocytogenes*

Kiyoshi Yoshimura, Ajay Jain, Heather E. Allen, et al.

Cancer Res 2006;66:1096-1104.